MICROWAVE IMAGING VIA SPACE-TIME BEAMFORMING FOR EARLY DETECTION OF BREAST CANCER

Essex J. Bond, Xu Li, Susan C. Hagness, and Barry D. Van Veen

Department of Electrical and Computer Engineering
University of Wisconsin-Madison, WI 53706 USA
e-mail: hagness@engr.wisc.edu

ABSTRACT

A backscatter-based microwave imaging technique that compensates for frequency-dependent propagation effects is proposed for detecting early-stage breast cancer. An array of antennas is located near the surface of the breast and an ultrawideband pulse is transmitted sequentially from each antenna. The received backscattered signals are passed through a space-time beamformer that is designed to image backscattered signal energy as a function of location. As a consequence of the significant dielectric-properties contrast between normal and malignant tissue, locations corresponding to malignant tumors are associated with large energy levels in the image. The effectiveness of these algorithms is demonstrated using simulated backscattered signals obtained from an anatomically realistic MRI-derived computational electromagnetic breast model. Very small (2 mm) malignant tumors embedded within the complex fibroglandular structure of the breast are easily detected above the background clutter.

1. INTRODUCTION

X-ray mammography, the most effective current method for detecting early stage breast cancer, suffers from relatively high false positive and negative rates, requires painful breast compression, and exposes the patient to low levels of ionizing radiation [1]. Microwave based imaging methods potentially overcome these limitations by exploiting the large dielectric properties contrast between normal and malignant tissue [2-4]. Both tomographic [5] and subsurface ultrawideband (UWB) radar techniques [6-8] have been proposed for detecting malignant lesions by exploiting dielectric-properties contrast. In microwave tomography, computational reconstruction algorithms are used to solve a nonlinear inverse-scattering problem and recover the dielectric-properties profile of the breast. The topic of this paper is UWB radar techniques, which seek to identify the presence and location of significant scatterers, that is, malignant lesions, in the breast. Successful adaptation of UWB radar techniques requires spatially focusing the backscattered signals to discriminate against clutter caused by the heterogeneity of normal breast tissue.

Previously proposed UWB radar approaches [6-8] are based on simple time shift and summing techniques and thus do not compensate for frequency-dependent propagation effects. In this paper we propose a method that explicitly compensates for frequency-dependent propagation effects through the use of space-time filtering. This enables detection of backscattered energy from small malignant breast tumors. Our method assumes the transmitted signals are ultrawideband pulses. The beamformer first time shifts the received signals and then passes them through a bank of finite-impulse response (FIR) filters. The FIR filter outputs are summed to produce the beamformer output. The weights in the FIR filters are designed using a least squares technique so that the beamformer passes the components of the backscattered signal originating from the candidate location with unit gain. The beamformer output is time gated, and the energy is calculated. A display of energy as a function of location provides an image of backscattered signal strength.

The following section of this paper describes our procedure for beamformer design using frequency-dependent propagation models. For ease of presentation we demonstrate our methods in two dimensions (2-D). The design of a 2-D beamformer is illustrated in Section 3. In Section 4, we present images of backscattered signal energy to illustrate the effectiveness of our algorithms.

2. MIST BEAMFORMING

The image of backscattered energy as a function of scan location $\mathbf{r}$ is obtained by applying a space-time beamformer designed for each scan location to the backscattered signals. The space-time beamformer for each scan location forms a weighted combination of time-delayed versions of the backscattered signals as shown in Figure 1. In this section, we consider the design of a space-time beamformer for a specific scan location $\mathbf{r}_0$. Our goal is to design the beamformer to pass backscattered signals from $\mathbf{r}_0$ with unit gain while attenuating signals from other locations [9].

For design purposes, we assume that the received signal in the i^{th} channel only contains the backscatter due to a lesion at location $\mathbf{r}_0$. In general, each received signal will contain contributions from the skin-breast interface, clutter due to heterogeneity in the breast, backscatter from possible lesions, and noise. The response from the skin-breast interface is much larger than the response from all other contributions and thus must be removed prior to performing tumor detection. One approach to removing the skin-breast artifact is to estimate the artifact as a filtered combination of the signal in all other channels [10]. In [10], we propose choosing the filter weights to minimize the residual mean-square error over that portion of the received data dominated by the reflection from the skin-breast interface.

Assuming the skin-breast artifact is removed, let the received signal in the i^{th} channel be denoted by $x_i[n]$ and its Fourier trans-

This work was supported by The Whitaker Foundation Biomedical Engineering Research Grant RG-99-0004. Computing resources were provided in part by Cray, Inc.

0-7803-7402-9/02/$17.00 ©2002 IEEE

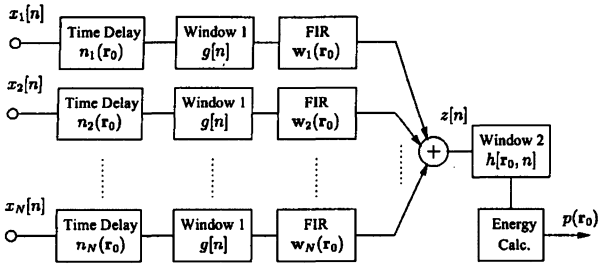

Fig. 1. Block diagram illustrating the MIST beamforming process for location $\mathbf{r}_0$ in the breast.

form denoted by

$$X_i(\omega) = I(\omega)S_{ii}(\mathbf{r}_0,\omega)\ , \qquad 1 \le i \le N \tag{1}$$

where $I(\omega)$ is the Fourier Transform of the transmitted pulse $i(t)$ and $S_{ii}(\mathbf{r}_0,\omega)$ is an analytical model of the monostatic frequency response associated with propagation through breast tissue from the i^{th} antenna to the scatterer located at $\mathbf{r}_0$ and back. $S_{ii}(\mathbf{r}_0,\omega)$ models the roundtrip time delay and dispersion for location $\mathbf{r}_0$.

The backscattered signal is delayed by an integer number of samples $n_i(\mathbf{r}_0) = n_a - \tau_i(\mathbf{r}_0)$ so that the waveforms in each channel are approximately aligned in time. Here $\tau_i(\mathbf{r}_0)$ denotes the roundtrip propagation delay for location $\mathbf{r}_0$ in the i^{th} channel, computed by dividing the roundtrip path length by the average speed of propagation and rounding to the nearest sample, and n_a is the reference time to which all received signals are aligned. We choose n_a as the worst case delay over all channels and locations,

$$n_a \ge \text{round}(\max_{i,\mathbf{r}_0} \tau_i(\mathbf{r}_0)) \tag{2}$$

The time aligned signals are windowed before the filtering stage to remove interference and clutter that is present prior to time n_a using the window function

$$g[n] = \begin{cases} 1 & n \ge n_a \\ 0 & \text{otherwise} \end{cases} \tag{3}$$

The purpose of the FIR filters is to equalize path length dependent dispersion and attenuation, interpolate any fractional time delays remaining in the backscattered lesion responses after coarse time alignment, and bandpass filter the signal. The FIR filter in the i^{th} channel has coefficients represented by the $L \times 1$ vector $\mathbf{w}_i$. The frequency response of the i^{th} filter is written as

$$W_i(\omega) = \sum_{\ell=0}^{L-1} w_{i\ell} e^{-j\omega\ell T_s} = \mathbf{w}_i^T \mathbf{d}(\omega) \tag{4}$$

where $\mathbf{w}_i^T = \left[w_{i0}, w_{i1}, \cdots, w_{i(L-1)}\right]$, T_s is the sampling interval, and $\mathbf{d}(\omega) = \left[\ 1, e^{-j\omega T_s}, \cdots, e^{-j\omega(L-1)T_s}\ \right]^T$. In order to pass signals from a location $\mathbf{r}_0$ with unit gain and a linear phase shift, we require

$$\sum_{i=1}^{N} S_{ii}(\mathbf{r}_0,\omega) e^{-j\omega n_i(\mathbf{r}_0)} W_i(\omega) =$$

$$\sum_{i=1}^{N} \widetilde{S}_{ii}(\mathbf{r}_0,\omega) e^{-j\omega\tau_i(\mathbf{r}_0)} e^{-j\omega n_i(\mathbf{r}_0)} \mathbf{w}_i^T \mathbf{d}(\omega)$$

$$\approx e^{-j\omega(T_s(L-1)/2 + n_a)} \tag{5}$$

Here $\widetilde{S}_{ii}(\mathbf{r}_0,\omega)$ represents dispersive effects - it is the frequency response due to propagation after removing the linear phase shift associated with roundtrip propagation delay, $\tau_i(\mathbf{r}_0)$. The quantity $T_s(L-1)/2$ in the last line of (5) represents the average time delay introduced by the FIR filters. Combining the phase factors associated with the propagation and the time alignment step according to $n_a = \tau_i(\mathbf{r}_0) + n_i(\mathbf{r}_0)$, we obtain the design constraints on $\mathbf{w}_i$ as

$$\sum_{i=1}^{N} \widetilde{S}_{ii}(\mathbf{r}_0,\omega) \mathbf{w}_i^T \mathbf{d}(\omega) \approx e^{-j\omega T_s(L-1)/2} \tag{6}$$

If these constraints are satisfied, then the summed output of the FIR filter bank, $z[n]$, has Fourier transform

$$Z(\omega) = I(\omega) e^{-j\omega(T_s(L-1)/2 + n_a)} \tag{7}$$

The output $z[n]$ is thus a time-shifted version of the transmitted pulse $i(t)$. Since $i(t)$ is localized in time, we window $z[n]$ with $h[\mathbf{r}_0, n]$ to eliminate additional clutter and compute the energy, $p(\mathbf{r}_0)$, by taking the sum of the squares of the windowed signal as follows:

$$p(\mathbf{r}_0) = \sum_n |z[n]h[\mathbf{r}_0, n]|^2 \tag{8}$$

The reconstructed image of microwave scattering strength is obtained by scanning $\mathbf{r}_0$ throughout the reconstruction region and plotting beamformer output energy as a function of location.

The following subsections describe details specific to the design of the filter weights $\mathbf{w}_i$ and the design of the window $h[\mathbf{r}_0, n]$.

2.1. Beamformer Design

Let the $NL \times 1$ filtering weight vector be $\mathbf{w} = \left[\ \mathbf{w}_1^T, \cdots, \mathbf{w}_N^T\ \right]^T$. We may rewrite (6) as

$$\mathbf{w}^T \mathbf{d}(\mathbf{r}_0,\omega) \approx e^{-j\omega T_s(L-1)/2} \tag{9}$$

where the $NL \times 1$ vector $\mathbf{d}(\mathbf{r}_0,\omega)$ is given by

$$\mathbf{d}(\mathbf{r}_0,\omega) = \left[\ \widetilde{S}_{11}^*(\mathbf{r}_0,\omega), \cdots, \widetilde{S}_{NN}^*(\mathbf{r}_0,\omega)\ \right]^H \otimes \mathbf{d}(\omega) \tag{10}$$

The symbol $\otimes$ denotes the Kronecker product operation. The filters are designed by seeking to approximate (9) on a dense grid of M distinct frequencies across the band $[\omega_\ell, \omega_u]$. To ensure that $\mathbf{w}$ is real-valued, we use positive and negative frequency pairs to construct the grid. Define a matrix containing the $\mathbf{d}(\mathbf{r}_0,\omega)$ at each of the M frequencies as

$$\mathbf{A} = \left[\ \mathbf{d}(\mathbf{r}_0,\omega_1), \cdots, \mathbf{d}(\mathbf{r}_0,\omega_M)\ \right] \tag{11}$$

Now (9) is expressed over the band $[\omega_\ell, \omega_u]$ as the system of M equations in NL unknowns

$$\mathbf{w}^T \mathbf{A} \approx \mathbf{f}_d \tag{12}$$

where

$$\mathbf{f}_d = \left[\ e^{-j\omega_1 T_s(L-1)/2}, \cdots, e^{-j\omega_M T_s(L-1)/2}\ \right] \tag{13}$$

Thus, the least squares design problem [9] for $\mathbf{w}$ is written as

$$\min_{\mathbf{w}} \left\| \mathbf{w}^T \mathbf{A} - \mathbf{f}_d \right\|_2^2 \tag{14}$$

The minimum-norm solution to this problem is

$$\mathbf{w} = (\mathbf{A}\mathbf{A}^H)^{-1}\mathbf{A}\mathbf{f}_d^H \tag{15}$$

The solution may have a very large norm if $\mathbf{A}$ is ill-conditioned. A large norm can cause the gain at locations other than $\mathbf{r}_0$ to become large and also amplify noise. In order to control these effects, we choose $\mathbf{w}$ as the solution to the penalized least squares problem

$$\min_{\mathbf{w}} \|\mathbf{w}^T \mathbf{A} - \mathbf{f}_d\|_2^2 + \lambda \|\mathbf{w}\|_2^2 \tag{16}$$

where λ is a constant chosen to trade the norm of $\mathbf{w}$ against the approximation error. The solution to (16) is

$$\mathbf{w} = (\mathbf{A}\mathbf{A}^H + \lambda \mathbf{I})^{-1}\mathbf{A}\mathbf{f}_d^H \tag{17}$$

2.2. Window Design

If the beamformer satisfies (6) and the lesion is a point scatterer, then the output $z[n]$ is a time-shifted, attenuated, and sampled version of the transmitted pulse $i(t)$. Both the time shift and pulse shape are known, so in this case the set of samples in $z[n]$ that contain backscattered signal from the tumor is known. If the backscattered signal occupies time points n_h through $n_h + \ell_h$ in $z[n]$, then a natural choice for the window is

$$h[\mathbf{r}_0, n] = \begin{cases} 1 & n_h \le n \le n_h + \ell_h \\ 0 & \text{otherwise} \end{cases} \tag{18}$$

This choice reduces clutter effects by ensuring that the output energy (8) is calculated using only samples of $z[n]$ containing backscattered lesion energy.

In practice, scattering from the tumor is frequency-dependent, so the backscattered signal is a distorted version of the transmitted pulse. These dispersive effects increase the duration of the backscattered signal and complicate window selection. Our preliminary investigations suggest that the extent of the increase in duration is directly proportional to the tumor size. Since we are interested in detecting very small lesions, we have chosen to design $h[\mathbf{r}_0, n]$ assuming a point scatterer model. This gives the largest possible signal to clutter ratio (S/C) for small tumors. The S/C for larger tumors is reduced by this choice; however, the backscattered signal from larger tumors is much stronger so a compromised S/C is relatively inconsequential for tumor detection. Note that tapered windows such as a raised cosine or decaying exponential could also be used to preserve signal energy while discriminating against clutter.

3. DESIGN OF A 2-D SPACE-TIME BEAMFORMER

In order to illustrate the MIST beamforming algorithm presented in Section 2, the design of a 2-D space-time beamformer will be discussed. We present the 2-D case to simplify the presentation; these techniques are directly applicable in three-dimensions (3-D). Frequency-dependent propagation effects are represented via the monostatic transfer function, $S_{ii}(\mathbf{r}, \omega)$, which relates the received signal at the i^{th} antenna to the transmitted signal at the i^{th} antenna due to a scatterer located at $\mathbf{r}$. To derive an analytic expression for

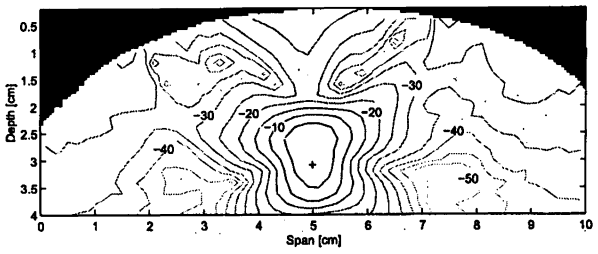

Fig. 2. Beamformer gain as a function of position in a 2-D plane of the breast for a design location at a span of 5.0 cm and a depth of 3.1 cm. The design location is marked by a '+'.

$S_{ii}(\mathbf{r}, \omega)$, we assume that each antenna is an infinite line source of electric current, $I(\omega)$, located in a uniform medium of normal breast tissue. The scatterer is treated as a conducting circular cylinder of radius a and infinite length. In our present design we assume that the scatterer has an infinitesimal radius compared to the small breast lesions we are interested in detecting.

Our 2-D beamformer is designed for a 1-D conformal antenna array containing 17 elements spanning 8 cm horizontally along the surface of the breast. The 2-D breast region through which the beamformer is designed to scan encompasses a span of 10 cm and a depth of 4 cm. The transmitted pulse is a differentiated Gaussian with a full width at half maximum equal to 110 ps. The spectrum of this pulse has a peak near 6 GHz and significant energy between 1 and 11 GHz. Therefore, the beamformer is designed over the range of frequencies of 1 to 11 GHz assuming a 50 GHz sampling frequency. The number of frequency samples used is $M = 1000$. The length of each FIR filter is $L = 45$. Both M and L are chosen so that (9) is approximately satisfied. The penalty parameter λ in (16) is set to 5. The design location $\mathbf{r}$ is scanned over the breast region using a grid resolution of 1 mm. The post-beamformer window described by (8) is six sampling intervals in length, spanning 120 ps.

Figure 2 illustrates the spatial discrimination capability of this 2-D beamformer with a plot of beamformer gain as a function of scatterer position on a dB scale for a beamformer designed to pass backscattered signals originating from the location (5.0 cm, 3.1 cm) with unit gain. This pattern shows that scattered signals originating from any location that is greater than 1 cm away from the design location are attenuated by more than 20 dB.

4. RESULTS

In this section we demonstrate the effectiveness of the MIST beamforming algorithms by applying them to backscatter signals obtained from an anatomically realistic numerical breast phantom. The phantom is derived from a high resolution MRI scan of a breast [8] and includes the heterogeneity due to complex fibroglandular tissue. The representative backscatter signals are computed using the finite-difference time-domain method of solving Maxwell's equations. It is assumed throughout this section that the algorithm described in [10] is applied to remove the skin-breast artifact from the backscatter signals. The beamformer for each scan location in the breast is applied to the backscatter signals, and the beamformer output energy is computed. Figures 3 and 4 present results when the beamformer output energy for each scan location is mapped into an image.

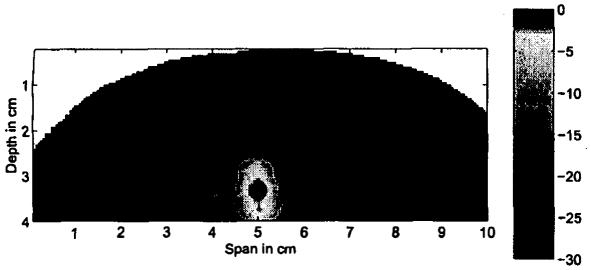

Fig. 3. Color image showing the backscattered energy for a numerical breast model with a 2-mm-diameter malignant tumor centered at (5.0 cm, 3.1 cm).

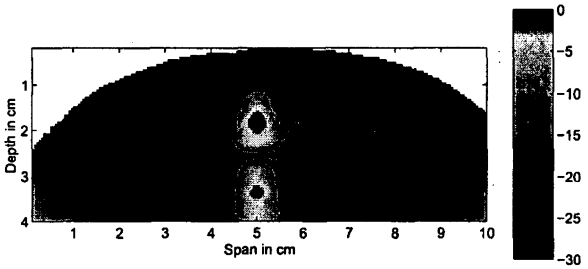

Fig. 4. Color image of backscattered energy for a numerical breast model with two 2-mm-diameter malignant tumors separated by 1.5 cm in the depth direction.

Figure 3 depicts the scanned beamformer output energy for the breast model that contains a 2-mm-diameter malignant tumor located at a depth of 3.1 cm. The origin of the dominant energy in this image, localized around (5.0 cm, 3.3 cm), is the dielectric-properties contrast between malignant and normal breast tissue. The low-level energy spatially distributed throughout the image is due to the heterogeneity of normal breast tissue in the numerical breast phantom. The tumor is clearly detectable as it stands 16 dB above the maximum clutter in a tumor-free model.

Figure 4 depicts the beamformer output energy for two adjacent 2-mm-diameter tumors separated by 1.5 cm with the deeper tumor located at a depth of 3.1 cm. Two distinct scattering objects are clearly evident. The tumor response closer to the skin has a S/C of 16 dB while the tumor response farther from the skin has a S/C of 15 dB. This example illustrates the resolving capability of MIST beamforming.

In each of the images of Figures 3 and 4, the peak of the tumor response occurs 2 to 3 mm deeper than the true center of the tumor. This small localization error is a consequence of assuming in the beamformer design that the scatterer is essentially a point-scatterer and of an inherent bias in the beamforming method toward deeper locations. The localization bias is due to the requirement that the beamformer compensate for attenuation.

5. CONCLUSIONS

A space-time beamforming method for imaging backscattered signal energy is proposed and demonstrated for detecting millimeter-sized malignant tumors in the breast. Our simulation results show that this method is exceptionally robust with respect to a number of potential challenges associated with imaging the inherently heterogeneous breast. Due to the enhanced synthetic-focusing capabilities of the MIST beamforming approach, the imaged backscatter from a 2-mm-diameter tumor stands out significantly above the clutter generated by the natural variations in the fibroglandular and adipose composition of the breast. Small lesions can be detected with high sensitivity regardless of location in the breast. The spatial selectivity of MIST beamforming also overcomes the challenge of detecting, localizing, and resolving multiple or multifocal lesions.

6. REFERENCES

[1] *Mammography and Beyond: Developing Techniques for the Early Detection of Breast Cancer*, Institute of Medicine, National Academy Press, Washington D.C., 2000.

[2] A. J. Surowiec, S. S. Stuchly, J. R. Barr, and A. Swarup, "Dielectric properties of breast carcinoma and the surrounding tissues," *IEEE Trans. Biomed. Eng.*, vol. 35, pp. 257–263, Apr. 1988.

[3] W. T. Joines, Y. Z. Dhenxing, and R. L. Jirtle, "The measured electrical properties of normal and malignant human tissues from 50 to 900 MHz," *Med. Phys.*, vol. 21, pp. 547–550, Apr. 1994.

[4] S. C. Hagness, X. Li, K. M. Leininger, J. H. Booske, and M. Okoniewski, "Dielectric characterization of human breast tissue and breast cancer detection algorithms for confocal microwave imaging," in *Microwaves: Theory and Applications in Materials Processing V*, D. E. Clark, J. G. P. Binner, and D. A. Lewis, eds., Westerville, OH: The American Ceramic Society, 2001.

[5] P. M. Meaney, M. W. Fanning, D. Li, S. P. Poplack, and K. D. Paulsen, "A clinical prototype for active microwave imaging of the breast," *IEEE Trans. Microwave Theory Tech.*, vol. 48, no. 11, pp. 1841–1853, Nov. 2000.

[6] S. C. Hagness, A. Taflove, and J. E. Bridges, "Two-dimensional FDTD analysis of a pulsed microwave confocal system for breast cancer detection: Fixed-focus and antenna-array sensors," *IEEE Trans. Biomed. Eng.*, vol. 45, no. 12, pp. 1470–1479, Dec. 1998.

[7] E. C. Fear and M. A. Stuchly, "Microwave detection of breast cancer," *IEEE Trans. Microwave Theory Tech.*, vol. 48, no. 11, pp. 1854–1863, Nov. 2000.

[8] X. Li and S. C. Hagness, "A confocal microwave imaging algorithm for breast cancer detection," *IEEE Microwave and Wireless Components Lett.*, vol. 11, no. 3, pp. 130–132, Mar. 2001.

[9] B. Van Veen, "Minimum variance beamforming," in *Adaptive Radar Detection and Estimation*, S. Haykin and A. Steinhardt, eds., Chapter 4, pp. 161–236. John Wiley and Sons, New York, 1992.

[10] E. J. Bond, X. Li, S. C. Hagness, and B. D. Van Veen, "Microwave Imaging via Space-Time Beamforming for Early Detection of Breast Cancer," *IEEE Trans. Antennas and Propagat.*, submitted.